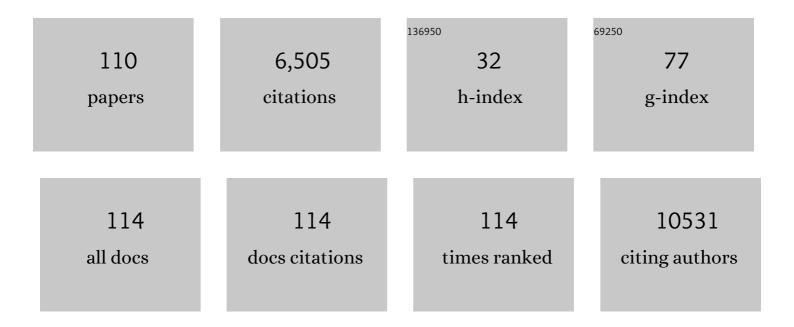


## List of Publications by Year in descending order

Source: https://exaly.com/author-pdf/92554/publications.pdf Version: 2024-02-01



Ro Hu

| #  | Article  | IF   | CITATIONS |
|----|--|------|-----------|
| 1  | Engineering Carbon Materials from the Hydrothermal Carbonization Process of Biomass. Advanced<br>Materials, 2010, 22, 813-828.   | 21.0 | 1,492     |
| 2  | Systemic Immune-Inflammation Index Predicts Prognosis of Patients after Curative Resection for Hepatocellular Carcinoma. Clinical Cancer Research, 2014, 20, 6212-6222.  | 7.0  | 1,012     |
| 3  | Large-Scale Synthesis of Flexible Free-Standing SERS Substrates with High Sensitivity: Electrospun PVA<br>Nanofibers Embedded with Controlled Alignment of Silver Nanoparticles. ACS Nano, 2009, 3, 3993-4002.                                   | 14.6 | 373       |
| 4  | Microwave-Assisted Rapid Facile "Green―Synthesis of Uniform Silver Nanoparticles: Self-Assembly into<br>Multilayered Films and Their Optical Properties. Journal of Physical Chemistry C, 2008, 112, 11169-11174.                                | 3.1  | 240       |
| 5  | Functional carbonaceous materials from hydrothermal carbonization of biomass: an effective chemical process. Dalton Transactions, 2008, , 5414.  | 3.3  | 196       |
| 6  | CD73 promotes hepatocellular carcinoma progression and metastasis via activating PI3K/AKT signaling by inducing Rap1-mediated membrane localization of P110β and predicts poor prognosis. Journal of Hematology and Oncology, 2019, 12, 37.      | 17.0 | 150       |
| 7  | Ordering of Disordered Nanowires: Spontaneous Formation of Highly Aligned, Ultralong Ag<br>Nanowire Films at Oil–Water–Air Interface. Advanced Functional Materials, 2010, 20, 958-964.  | 14.9 | 139       |
| 8  | <i>In Situ</i> Growth Strategy to Integrate Up-Conversion Nanoparticles with Ultrasmall CuS for Photothermal Theranostics. ACS Nano, 2017, 11, 1064-1072.  | 14.6 | 132       |
| 9  | Circulating Tumor Cells from Different Vascular Sites Exhibit Spatial Heterogeneity in Epithelial and<br>Mesenchymal Composition and Distinct Clinical Significance in Hepatocellular Carcinoma. Clinical<br>Cancer Research, 2018, 24, 547-559. | 7.0  | 112       |
| 10 | Circulating Tumor Cells with Stem-Like Phenotypes for Diagnosis, Prognosis, and Therapeutic<br>Response Evaluation in Hepatocellular Carcinoma. Clinical Cancer Research, 2018, 24, 2203-2213.   | 7.0  | 102       |
| 11 | Avoiding Thiol Compound Interference: A Nanoplatform Based on Highâ€Fidelity Au–Se Bonds for<br>Biological Applications. Angewandte Chemie - International Edition, 2018, 57, 5306-5309.   | 13.8 | 100       |
| 12 | Clinical Significance of <i>EpCAM</i> mRNA-Positive Circulating Tumor Cells in Hepatocellular<br>Carcinoma by an Optimized Negative Enrichment and qRT-PCR–Based Platform. Clinical Cancer<br>Research, 2014, 20, 4794-4805.                     | 7.0  | 99        |
| 13 | Uniformly Shaped Poly( <i>p</i> â€phenylenediamine) Microparticles: Shapeâ€controlled Synthesis and<br>Their Potential Application for the Removal of Lead Ions from Water. Advanced Functional Materials,<br>2008, 18, 1105-1111.               | 14.9 | 96        |
| 14 | Size-controllable palladium nanoparticles immobilized on carbon nanospheres for nitroaromatic<br>hydrogenation. Journal of Materials Chemistry A, 2013, 1, 3783.   | 10.3 | 92        |
| 15 | An Ultrasensitive Cyclizationâ€Based Fluorescent Probe for Imaging Native HOBr in Live Cells and<br>Zebrafish. Angewandte Chemie - International Edition, 2016, 55, 12751-12754.   | 13.8 | 90        |
| 16 | Dissecting spatial heterogeneity and the immune-evasion mechanism of CTCs by single-cell RNA-seq in hepatocellular carcinoma. Nature Communications, 2021, 12, 4091.   | 12.8 | 90        |
| 17 | Microwave-assisted synthesis of silver indium tungsten oxide mesocrystals and their selective photocatalytic properties. Chemical Communications, 2010, 46, 2277.  | 4.1  | 79        |
| 18 | Sphere-forming culture enriches liver cancer stem cells and reveals Stearoyl-CoA desaturase 1 as a potential therapeutic target. BMC Cancer, 2019, 19, 760.  | 2.6  | 78        |

| #  | Article  | IF   | CITATIONS |
|----|--|------|-----------|
| 19 | Mesocrystals of Rutile TiO <sub>2</sub> : Mesoscale Transformation, Crystallization, and Growth by a<br>Biologic Molecules-Assisted Hydrothermal Process. Crystal Growth and Design, 2009, 9, 203-209.   | 3.0  | 75        |
| 20 | High Upconversion Efficiency from Hetero Triplet–Triplet Annihilation in Multiacceptor Systems.<br>Journal of Physical Chemistry Letters, 2013, 4, 2334-2338.  | 4.6  | 75        |
| 21 | Au–Se-Bond-Based Nanoprobe for Imaging MMP-2 in Tumor Cells under a High-Thiol Environment.<br>Analytical Chemistry, 2018, 90, 4719-4724.  | 6.5  | 67        |
| 22 | Anlotinib suppresses tumor progression via blocking the VEGFR2/PI3K/AKT cascade in intrahepatic cholangiocarcinoma. Cell Death and Disease, 2020, 11, 573.   | 6.3  | 65        |
| 23 | A polymeric nanoparticle formulation of curcumin in combination with sorafenib synergistically<br>inhibits tumor growth and metastasis in an orthotopic model of human hepatocellular carcinoma.<br>Biochemical and Biophysical Research Communications, 2015, 468, 525-532. | 2.1  | 59        |
| 24 | Selective Chromogenic Detection of Thiol-Containing Biomolecules Using Carbonaceous Nanospheres<br>Loaded with Silver Nanoparticles as Carrier. ACS Nano, 2011, 5, 3166-3171.  | 14.6 | 56        |
| 25 | An Ultrasensitive Cyclizationâ€Based Fluorescent Probe for Imaging Native HOBr in Live Cells and<br>Zebrafish. Angewandte Chemie, 2016, 128, 12943-12946.  | 2.0  | 56        |
| 26 | Circulating CD14 <sup>+</sup> HLAâ€DR <sup>â^'/low</sup> myeloidâ€derived suppressor cells predicted<br>early recurrence of hepatocellular carcinoma after surgery. Hepatology Research, 2017, 47, 1061-1071.  | 3.4  | 56        |
| 27 | Surface plasmon-photosensitizer resonance coupling: an enhanced singlet oxygen production<br>platform for broad-spectrum photodynamic inactivation of bacteria. Journal of Materials Chemistry<br>B, 2014, 2, 7073-7081.   | 5.8  | 46        |
| 28 | Apolipoprotein A1: a novel serum biomarker for predicting the prognosis of hepatocellular carcinoma after curative resection. Oncotarget, 2016, 7, 70654-70668.  | 1.8  | 44        |
| 29 | Selective colorimetric detection of glutathione based on quasi-stable gold nanoparticles assembly.<br>New Journal of Chemistry, 2013, 37, 3853.  | 2.8  | 43        |
| 30 | Polymeric immunoglobulin receptor promotes tumor growth in hepatocellular carcinoma.<br>Hepatology, 2017, 65, 1948-1962.   | 7.3  | 43        |
| 31 | Unique Lamellar Sodium/Potassium Iron Oxide Nanosheets: Facile Microwave-Assisted Synthesis and<br>Magnetic and Electrochemical Properties. Chemistry of Materials, 2011, 23, 3946-3952.   | 6.7  | 42        |
| 32 | Real-Time in Situ Visualizing of the Sequential Activation of Caspase Cascade Using a Multicolor<br>Gold–Selenium Bonding Fluorescent Nanoprobe. Analytical Chemistry, 2019, 91, 5994-6002.  | 6.5  | 41        |
| 33 | Droplet-based PCR in a 3D-printed microfluidic chip for miRNA-21 detection. Analytical Methods, 2019, 11, 3286-3293.   | 2.7  | 33        |
| 34 | Circulating microRNA-422a is associated with lymphatic metastasis in lung cancer. Oncotarget, 2017, 8,<br>42173-42188.   | 1.8  | 33        |
| 35 | Dynamic Liquid Surface Enhanced Raman Scattering Platform Based on Soft Tubular Microfluidics for<br>Label-Free Cell Detection. Analytical Chemistry, 2019, 91, 7973-7979.   | 6.5  | 32        |
| 36 | Detection of circulating tumour cells enables early recurrence prediction in hepatocellular carcinoma patients undergoing liver transplantation. Liver International, 2021, 41, 562-573.   | 3.9  | 32        |

| #  | Article   | IF   | CITATIONS |
|----|---|------|-----------|
| 37 | Controllable Synthesis of Zincâ€Substituted α―and βâ€Nickel Hydroxide Nanostructures and Their Collective<br>Intrinsic Properties. Chemistry - A European Journal, 2008, 14, 8928-8938.   | 3.3  | 31        |
| 38 | Simultaneous fluorescence imaging of selenol and hydrogen peroxide under normoxia and hypoxia in<br>HepG2 cells and in vivo. Chemical Communications, 2016, 52, 6693-6696.  | 4.1  | 31        |
| 39 | A nanosensor for inÂvivo selenol imaging based on the formation of Au Se bonds. Biomaterials, 2016,<br>92, 81-89.   | 11.4 | 30        |
| 40 | Long non-coding RNA00364 represses hepatocellular carcinoma cell proliferation via modulating p-STAT3-IFIT2 signaling axis. Oncotarget, 2017, 8, 102006-102019.   | 1.8  | 30        |
| 41 | Novel Anatase TiO <sub>2</sub> Boxes and Tree-like Structures Assembled by Hollow Tubes:<br><scp>d</scp> , <scp>l</scp> -Malic Acid-Assisted Hydrothermal Synthesis, Growth Mechanism, and<br>Photocatalytic Properties. Crystal Growth and Design, 2009, 9, 1511-1518. | 3.0  | 29        |
| 42 | Plasmon-enhanced homogeneous and heterogeneous triplet–triplet annihilation by gold<br>nanoparticles. Physical Chemistry Chemical Physics, 2015, 17, 14479-14483.   | 2.8  | 29        |
| 43 | HOXB7 promotes tumor progression via bFGF-induced activation of MAPK/ERK pathway and indicated poor prognosis in hepatocellular carcinoma. Oncotarget, 2017, 8, 47121-47135.  | 1.8  | 29        |
| 44 | KPNA3 Confers Sorafenib Resistance to Advanced Hepatocellular Carcinoma via TWIST Regulated<br>Epithelial-Mesenchymal Transition. Journal of Cancer, 2019, 10, 3914-3925.   | 2.5  | 27        |
| 45 | Application of Serum Annexin A3 in Diagnosis, Outcome Prediction and Therapeutic Response<br>Evaluation for Patients with Hepatocellular Carcinoma. Annals of Surgical Oncology, 2018, 25,<br>1686-1694.  | 1.5  | 25        |
| 46 | Syringe pump-assisted synthesis of water-soluble cubic structure Ag2Se nanocrystals by a cation-exchange reaction. Journal of Colloid and Interface Science, 2008, 325, 351-355.  | 9.4  | 24        |
| 47 | Ascorbic acid induced HepG2 cells' apoptosis <i>via</i> intracellular reductive stress. Theranostics, 2019, 9, 4233-4240.   | 10.0 | 24        |
| 48 | Intelligent Control Strategy for Transient Response of a Variable Geometry Turbocharger System<br>Based on Deep Reinforcement Learning. Processes, 2019, 7, 601.  | 2.8  | 24        |
| 49 | Highly Erbium-Doped Nanoplatform with Enhanced Red Emission for Dual-Modal<br>Optical-Imaging-Guided Photodynamic Therapy. Inorganic Chemistry, 2018, 57, 14594-14602.  | 4.0  | 23        |
| 50 | Effect of surgical margin on recurrence based on preoperative circulating tumor cell status in hepatocellular carcinoma. EBioMedicine, 2020, 62, 103107.  | 6.1  | 23        |
| 51 | Hierarchical silver indium tungsten oxide mesocrystals with morphology-, pressure-, and temperature-dependent luminescence properties. Nano Research, 2010, 3, 395-403.   | 10.4 | 22        |
| 52 | Avoiding Thiol Compound Interference: A Nanoplatform Based on Highâ€Fidelity Au–Se Bonds for<br>Biological Applications. Angewandte Chemie, 2018, 130, 5404-5407.   | 2.0  | 22        |
| 53 | Promyelocytic leukemia protein induces arsenic trioxide resistance through regulation of aldehyde dehydrogenase 3 family member A1 in hepatocellular carcinoma. Cancer Letters, 2015, 366, 112-122.   | 7.2  | 21        |
| 54 | Tumour-suppressive role of PTPN13 in hepatocellular carcinoma and its clinical significance. Tumor<br>Biology, 2016, 37, 9691-9698.   | 1.8  | 20        |

| #  | Article  | IF   | CITATIONS |
|----|--|------|-----------|
| 55 | PARG inhibition limits HCC progression and potentiates the efficacy of immune checkpoint therapy.<br>Journal of Hepatology, 2022, 77, 140-151.   | 3.7  | 20        |
| 56 | Engineering of Removing Sacrificial Materials in 3D-Printed Microfluidics. Micromachines, 2018, 9, 327.  | 2.9  | 19        |
| 57 | Shanghai Score. Chinese Medical Journal, 2017, 130, 2650-2660.   | 2.3  | 18        |
| 58 | A review of recent advancements in Ni-related materials used for microwave absorption. Journal Physics D: Applied Physics, 2021, 54, 473003.   | 2.8  | 18        |
| 59 | 3D-Printed Concentration-Controlled Microfluidic Chip with Diffusion Mixing Pattern for the Synthesis of Alginate Drug Delivery Microgels. Nanomaterials, 2019, 9, 1451.   | 4.1  | 17        |
| 60 | Porous nanocomposite membranes based on functional GO with selective function for lithium adsorption. New Journal of Chemistry, 2018, 42, 4432-4442.   | 2.8  | 16        |
| 61 | Shifting Deep Reinforcement Learning Algorithm Toward Training Directly in Transient Real-World<br>Environment: A Case Study in Powertrain Control. IEEE Transactions on Industrial Informatics, 2021,<br>17, 8198-8206.                           | 11.3 | 16        |
| 62 | TGM3 promotes epithelial–mesenchymal transition and hepatocellular carcinogenesis and predicts poor prognosis for patients after curative resection. Digestive and Liver Disease, 2020, 52, 668-676.   | 0.9  | 15        |
| 63 | MicroRNA-19a-3p regulates cell growth through modulation of the PIK3IP1-AKT pathway in hepatocellular carcinoma. Journal of Cancer, 2020, 11, 2476-2484.   | 2.5  | 15        |
| 64 | A fluorescent molecularly imprinted polymer sensor synthesized by atom transfer radical precipitation polymerization for determination of ultra trace fenvalerate in the environment. RSC Advances, 2016, 6, 81346-81353.                          | 3.6  | 13        |
| 65 | River meander-inspired cross-section in 3D-printed helical microchannels for inertial focusing and enrichment. Sensors and Actuators B: Chemical, 2019, 301, 127125.   | 7.8  | 13        |
| 66 | Far upstream element-binding protein 1 facilitates hepatocellular carcinoma invasion and metastasis.<br>Carcinogenesis, 2020, 41, 950-960.   | 2.8  | 13        |
| 67 | Simulation and practice of particle inertial focusing in 3D-printed serpentine microfluidic chips <i>via</i> commercial 3D-printers. Soft Matter, 2020, 16, 3096-3105.   | 2.7  | 13        |
| 68 | CD155/SRC complex promotes hepatocellular carcinoma progression via inhibiting the p38 MAPK signalling pathway and correlates with poor prognosis. Clinical and Translational Medicine, 2022, 12, e794.  | 4.0  | 13        |
| 69 | Constructing porous intramolecular donor–acceptor integrated carbon nitride doped with<br><i>m</i> -aminophenol for boosting photocatalytic degradation and hydrogen evolution activity.<br>Catalysis Science and Technology, 2022, 12, 4591-4604. | 4.1  | 13        |
| 70 | An Adaptive Hierarchical Energy Management Strategy for Hybrid Electric Vehicles Combining<br>Heuristic Domain Knowledge and Data-Driven Deep Reinforcement Learning. IEEE Transactions on<br>Transportation Electrification, 2022, 8, 3275-3288.  | 7.8  | 12        |
| 71 | Differentially expressed miRNAs in hepatocellular carcinoma cells under hypoxic conditions are associated with transcription and phosphorylation. Oncology Letters, 2017, 15, 467-474.   | 1.8  | 11        |
| 72 | Eight Hundred Years of Drought and Flood Disasters and Precipitation Sequence Reconstruction in<br>Wuzhou City, Southwest China. Water (Switzerland), 2019, 11, 219.   | 2.7  | 11        |

| #  | Article   | IF   | CITATIONS |
|----|---|------|-----------|
| 73 | BCL11B suppresses tumor progression and stem cell traits in hepatocellular carcinoma by restoring p53 signaling activity. Cell Death and Disease, 2020, 11, 895.  | 6.3  | 11        |
| 74 | Zwitterion imprinted composite membranes with obvious antifouling character for selective separation of Li ions. Korean Journal of Chemical Engineering, 2020, 37, 707-715.   | 2.7  | 11        |
| 75 | Facile PEG-based isolation and classification of cancer extracellular vesicles and particles with<br>label-free surface-enhanced Raman scattering and pattern recognition algorithm. Analyst, The, 2021,<br>146, 1949-1955.             | 3.5  | 11        |
| 76 | Drug preconcentration and direct quantification in biofluids using 3D-Printed paper cartridge.<br>Biosensors and Bioelectronics, 2021, 189, 113266.   | 10.1 | 11        |
| 77 | Simultaneously Enhanced Singlet Oxygen and Fluorescence Production of Nanoplatform by Surface<br>Plasmon Resonance Coupling for Biomedical Applications. Langmuir, 2019, 35, 14833-14839.   | 3.5  | 10        |
| 78 | Clinical Characteristics and Prognostic Factors of Patients with Intrahepatic Cholangiocarcinoma with Fever: A Propensity Score Matching Analysis. Oncologist, 2019, 24, 997-1007.  | 3.7  | 9         |
| 79 | Plasmonic modulated upconversion fluorescence by adjustable distributed gold nanoparticles.<br>Journal of Luminescence, 2020, 220, 116974.  | 3.1  | 9         |
| 80 | Monitoring the Activation of Caspases-1/3/4 for Describing the Pyroptosis Pathways of Cancer Cells.<br>Analytical Chemistry, 2021, 93, 12022-12031.   | 6.5  | 9         |
| 81 | Targetable Mesoporous Silica Nanoprobes for Mapping the Subcellular Distribution of<br>H <sub>2</sub> Se in Cancer Cells. ACS Applied Materials & Interfaces, 2018, 10, 17345-17351.  | 8.0  | 8         |
| 82 | Elevated soluble programmed death-ligand 1 levels indicate immunosuppression and poor prognosis in<br>hepatocellular carcinoma patients undergoing transcatheter arterial chemoembolization. Clinica<br>Chimica Acta, 2020, 511, 67-74. | 1.1  | 8         |
| 83 | Mucin 1 promotes tumor progression through activating WNT/β-catenin signaling pathway in intrahepatic cholangiocarcinoma. Journal of Cancer, 2021, 12, 6937-6947.   | 2.5  | 8         |
| 84 | Excitation of surface plasmons in a single silver nanowire using higher-order-mode light. Physica E:<br>Low-Dimensional Systems and Nanostructures, 2010, 42, 1751-1754.  | 2.7  | 7         |
| 85 | Electronic, Optical, and Charge Transport Properties of New 2,1,3-Benzothiadiazole-Based Derivative for Organic Light-Emitting Diodes. Spectroscopy Letters, 2012, 45, 17-21.   | 1.0  | 7         |
| 86 | Non-powered capillary force-driven stamped approach for directly printing nanomaterials aqueous solution on paper substrate. Lab on A Chip, 2020, 20, 931-941.  | 6.0  | 7         |
| 87 | Mineralization of calcite ribbons on an Allium fistulosum L. bulb inner membrane in an<br>ethanol–water mixed solvent under control of polyacrylic acid by a double diffusion method.<br>CrystEngComm, 2010, 12, 3593.                  | 2.6  | 6         |
| 88 | Dual Control of Interparticle Forces in Assembly of Gold Nanoparticles. ChemPlusChem, 2013, 78, 506-514.  | 2.8  | 6         |
| 89 | Lightâ€Harvesting Photosensitizers for Photodynamic Inactivation of Bacteria under Both Visible and<br>Nearâ€Infrared Excitations. Chemistry - an Asian Journal, 2016, 11, 1092-1097.   | 3.3  | 5         |
| 90 | Elastoplastic Deformation of Silk Micro- and Nanostructures. ACS Biomaterials Science and Engineering, 2016, 2, 893-899.  | 5.2  | 5         |

| #   | Article   | IF  | CITATIONS |
|-----|---|-----|-----------|
| 91  | Magnetic anomaly characteristics of surface crack defects in a titanium alloy plate. Nondestructive Testing and Evaluation, 2021, 36, 209-224.  | 2.1 | 5         |
| 92  | Smartphone-Based Quantitative Fluorescence Detection of Flowing Droplets Using Embedded Ambient<br>Light Sensor. IEEE Sensors Journal, 2021, 21, 4451-4461.   | 4.7 | 5         |
| 93  | Removal of Sulfadiazine by Polyamide Nanofiltration Membranes: Measurement, Modeling, and<br>Mechanisms. Membranes, 2021, 11, 104.  | 3.0 | 5         |
| 94  | Patient-Derived Xenograft Models for Intrahepatic Cholangiocarcinoma and Their Application in Guiding Personalized Medicine. Frontiers in Oncology, 2021, 11, 704042.   | 2.8 | 5         |
| 95  | Detecting QTL and Candidate Genes for Plant Height in Soybean via Linkage Analysis and GWAS.<br>Frontiers in Plant Science, 2021, 12, 803820.   | 3.6 | 5         |
| 96  | Dynamic response of aluminum honeycomb sandwich panels subjected to hypervelocity impact by porous volcanic rock projectile. Journal of Mechanical Science and Technology, 2019, 33, 2605-2616.   | 1.5 | 4         |
| 97  | Simultaneous bioimaging of MMP-2 and MMP-7 via Au-Se constructed fluorescence nanoprobe. Science China Chemistry, 2020, 63, 135-140.  | 8.2 | 4         |
| 98  | A plug-and-play 3D hydrodynamic focusing Raman platform for label-free and dynamic single microparticle detection. Sensors and Actuators B: Chemical, 2022, 369, 132273.  | 7.8 | 4         |
| 99  | Anomalous dielectric behaviors of electrolyte solutions confined in graphene oxide nanochannels.<br>Scientific Reports, 2021, 11, 18689.  | 3.3 | 3         |
| 100 | Se-modified gold nanorods for enhancing the efficiency of photothermal therapy: avoiding the off-target problem induced by biothiols. Journal of Materials Chemistry B, 2021, 9, 8832-8841.   | 5.8 | 3         |
| 101 | Differential network analysis depicts regulatory mechanisms for hepatocellular carcinoma from diverse backgrounds. Future Oncology, 2019, 15, 3917-3934.  | 2.4 | 2         |
| 102 | QTL for Main Stem Node Number and Its Response to Plant Densities in 144 Soybean FW-RILs. Frontiers<br>in Plant Science, 2021, 12, 666796.  | 3.6 | 2         |
| 103 | Biological Characteristics of Cell Similarity Measure. Advanced Intelligent Systems, 2022, 4, 2100093.  | 6.1 | 2         |
| 104 | Acid-driven aggregation of selenol-functionalized zwitterionic gold nanoparticles improves the photothermal treatment efficacy of tumors. Materials Chemistry Frontiers, 2022, 6, 775-782.  | 5.9 | 2         |
| 105 | ELECTRON-WITHDRAWING SUBSTITUTED BTD-BASED DERIVATIVE: ELECTRONIC AND OPTICAL PROPERTIES, CHARGE TRANSFER, STABILITY STUDY. Journal of Theoretical and Computational Chemistry, 2011, 10, 829-838.  | 1.8 | 1         |
| 106 | Magnetic testing for inter-granular crack defect of tubing coupling. Nondestructive Testing and Evaluation, 2018, 33, 119-129.  | 2.1 | 1         |
| 107 | Comparison of immune profiles between hepatocellular carcinoma subtypes. Biophysics Reports, 2020,<br>6, 19-32.   | 0.8 | 1         |
| 108 | Reply to the â€~Comment on "Investigation of dielectric constants of water in a nano-confined poreâ€â€™ by<br>S. Mondal and B. Bagchi, <i>RSC Adv.</i> , 2020, <b>10</b> , DOI: 10.1039/D0RA02726J. RSC Advances, 2021,<br>11, 5753-5754. | 3.6 | 1         |

| #   | Article   | IF  | CITATIONS |
|-----|---|-----|-----------|
| 109 | Evaluation of Fatigue Damage in 304 Stainless Steel by Measuring Residual Magnetic Field. Studies in<br>Applied Electromagnetics and Mechanics, 2020, , .         | 0.2 | 1         |
| 110 | Dielectric Properties of Aqueous Electrolyte Solutions Confined in Silica Nanopore: Molecular<br>Simulation vs. Continuum-Based Models. Membranes, 2022, 12, 220. | 3.0 | 0         |